BIOELECTRICITY
Volume 2, Number 2, 2020

DOI: 10.1089/bioe.2020.0015

Original Research

Differential Cell Death and Regrowth of Dermal Fibroblasts and Keratinocytes After Application of Pulsed Electric Fields

Bodhisatwa Das, PhD,[1] Anil Shrirao, PhD,[1] Alexander Golberg, PhD,[2] Francois Berthiaume, PhD,[1] Rene Schloss, PhD,[1] and Martin L. Yarmush, MD, PhD[1,3,4]

Abstract

Background: High-powered pulsed electric fields (PEF) may be used for tissue debridement and disinfection, while lower PEF intensities may stimulate beneficial cellular responses for wound healing. We investigated the dual effects of nonuniform PEF on cellular death and stimulation.
Methods: Dermal fibroblast or keratinocyte monolayers were exposed to PEF induced by two needle electrodes (2 mm apart). Voltages (100–600 V; 1 Hz; 70 micros pulse width; 90 pulses/cycle) were applied between the two electrodes. Controls consisted of similar monolayers subjected to a scratch mechanical injury.
Results: Cell growth and closure of the cell-free gap was faster in PEF-treated cell monolayers versus scratched ones. Media conditioned from cells pre-exposed to PEF, when applied to responder cells, stimulated greater proliferation than media from scratched monolayers.
Conclusions: PEF treatment causes the release of soluble factors that promote cell growth, and thus may play a role in the accelerated healing of wounds post PEF.

Keywords: skin, wound healing, pulsed electric fields

Introduction

Pulsed electric fields (PEF) have been utilized for a large number of biological applications, including food disinfection, cloning, gene silencing, and drug and other biomolecule delivery.[1–4] It is thought that PEF achieves nonthermal cell death mainly through rapid alteration of the resting membrane potential of the target cells, leading to irreversible generation of nanopores (irreversible electroporation or IRE) and rupture of the cells.[5] In general, PEF parameter selection for specific applications encompasses electric field strength, pulse number, duration, frequency, and polarity.[6–8] Recently, health care engineering has explored this highly interesting biophysical technique for a number of therapeutic purposes.[9,10]

Another area where PEF have been explored is for wound healing and related therapies; for example, PEF-induced IRE can be a highly effective technique to disinfect burn injuries.[11,12] It can also assist in the disinfection of antibiotic-resistant biofilm-forming bacterial colonies to restore the wound healing process.[13] It is postulated that IRE can kill cells at the injury site without degrading the native extracellular matrix architecture.[14] By preserving the native tissue scaffold, cells can migrate into the injuiry site and may even lead to scarless wound healing.[15–17] Although it has been proposed that IRE enhances blood flow into the surrounding tissue, the molecular and cellular mechanisms behind improved healing are unclear.[18]

While a lethal dose of high-intensity pulses is utilized for massive cellular destruction and as an alternative to surgical debridement, PEF has also been explored for electrostimulation in wound healing; for example, it has been hypothesized that PEF may guide stem cells toward injured dermal tissue.[19–22] Low-voltage electrostimulation has been found to alter regenerative gene expression in keratinocytes, and electric fields have been found[23] to enhance migration and influence directionality of keratinocytes.[24] PEF also have been observed to affect the prolifrtation and differentiation pattern of hematopoetic stem cells, osteoblasts, and myoblasts.[25,26]

In most health care applications of PEF, studies only focus on a single mode of PEF application, either stimulation or tissue ablation.[11,16] Herein, we explored the combined effect of PEF on cell death and cell growth stimulation in two major skin cell types (human dermal fibroblasts and keratinocytes).

[1]Department of Biomedical Engineering, Rutgers University, Piscataway, New Jersey, USA.
[2]Department of Environmental Studies, Tel Aviv University, Tel Aviv, Israel.
[3]Center for Engineering in Medicine, Massachusetts General Hospital, Boston, Massachusetts, USA.
[4]Shriners Hospitals for Children, Boston, Massachusetts, USA.

The data suggest that PEF results in a dual effect of IRE-induced cell death and release of soluble factors that stimulate remaining viable cells.

Materials and Methods

All cells were cultured in Dulbecco's modified Eagle's medium (with 4.5 g/L glucose; Gibco) supplemented with 1% Penicillin–Streptomycin solution (Gibco) and 5% fetal bovine serum (Gibco) in an incubator at 37°C and in the presence of 5% CO_2 and controlled humidity. Human dermal fibroblasts (passages 3–5) and keratinocytes (HaCaT cells, passages 38–42) were used for *in vitro* cell culture studies. For cell washing purposes, phosphate-buffered saline (PBS; Gibco) was utilized. A BTX extracellular matrix (ECM) 830 (Harvard Apparatus) was utilized for electroporation studies. High impedance electroporation buffer (from BTX) was used to prevent short circuits and sparks, and isolate a conduction path through the cell monolayer.

Experimental setup for PEF application

PEF application was aided by a machined template cover with guiding holes (1 mm apart) for inserting needle electrodes (600 μm diameter) at specified locations inside individual wells of a 24-well plate. (Fig. 1A, B). PEF was applied by a BTX ECM 830 square wave electroporator.

Cell monolayer recovery after injury by PEF

For this study, 1×10^5 cells/well (fibroblasts or keratinocytes), were seeded in 24-well plates and allowed to grow to confluence for 72 h. Cell culture medium was removed, cells washed with PBS, and electroporation medium was added to the well. After PEF treatment, the electroporation medium was removed, the cells were washed with PBS, and fresh medium was added. Voltages ranging from 100 to 600 V were applied between the two electrodes (2 mm apart edge to edge), while the other PEF parameters (1 Hz; 70 μs pulse width; 90 pulses per cycle, 1 cycle applied for each sample) remained constant (Fig. 1C).

Wells were imaged by phase contrast (2 × magnification, EVOS cell imaging system; Thermo Scientific), before PEF application, and then at various time points extending up to 120 h post-PEF. Fibroblast controls consisted of monolayers subjected to a similar-sized mechanical scratch injury (as of post PEF application in the voltage range 500–600 V) created using a micropipette tip. Keratinocyte controls also consisted of mechanical scratch injuries but the area was made to match the injury area of PEF application (500–600 V) post 24 h, due to delayed cell death observed in this cell type after PEF. The studies were run in quadruplicate and monolayer recovery was monitored daily up to 96 h.

Images were analyzed using ImageJ software to determine average area and diameter of the cell-free zone (corresponding to the injury). These values were measured and plotted as mean ± standard deviation versus time using Origin Pro-8 software. To analyze recovery curves, straight lines were fitted to the curves taking all the regions of the curve into consideration to obtain the average slope and intercepts. Slope measurement was conducted from the linear fit of the area recovery curves. The slope values were plotted using negative *Y*-axis for both fibroblasts and keratinocytes as the original curves had negative slopes due to area shrinkage from high to low. The slope measurement plots represent the rate of recovery of the injuries in different voltage applications with respect to controls. We also measured the

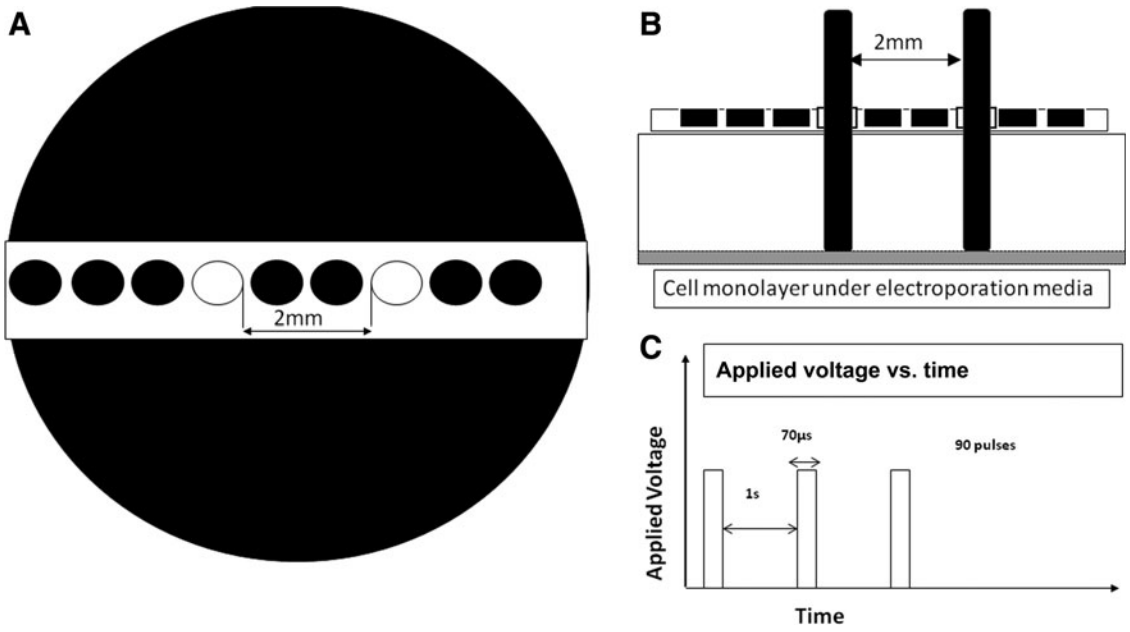

FIG. 1. *In vitro* customized electrode guiding system designed to fit 24-well plates. **(A)** Top view of guide covered well where black holes remain open and the two white holes are the ones used here for needle insertion (needle electrode 600 μm diameter), with an edge-to-edge distance of 2 mm. **(B)** Side view of poly acrylic guide with electrodes inserted in two holes 2 mm apart. The bottom of the needle electrodes reaches the level of cellular monolayer through the electroporation media. **(C)** Representative PEF waveforms showing pulse width, duration between pulses, and number of pulses (note that pulse width is not to scale). PEF, pulsed electric fields.

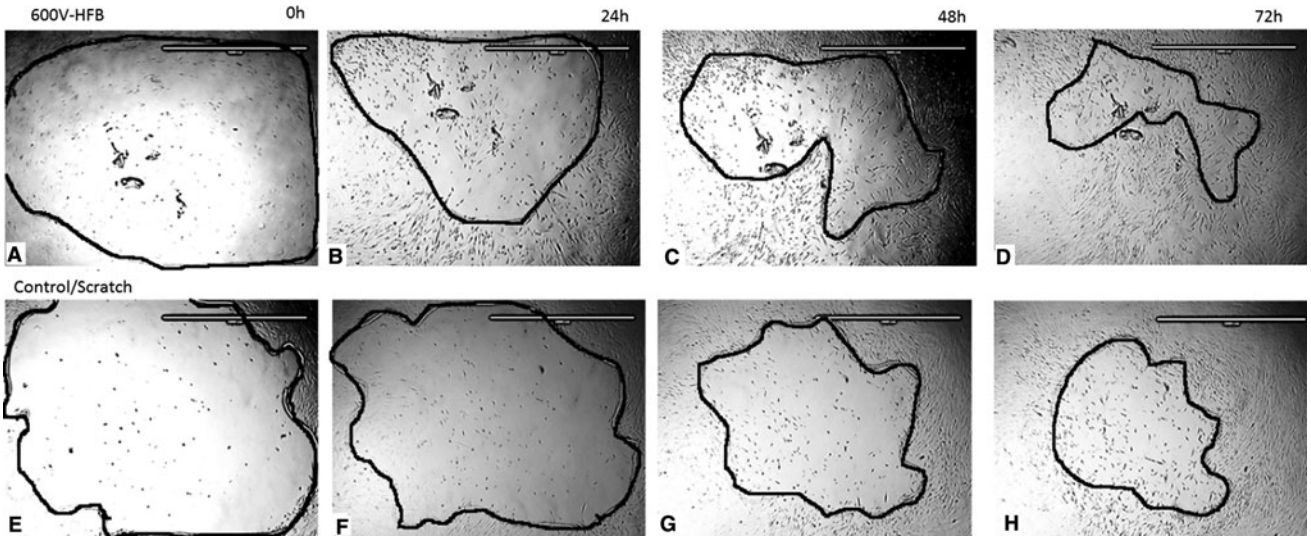

FIG. 2. Injury recovery of human fibroblast (HFB) monolayers after treatment with 600 V PEF between 2 mm, or after mechanical scratching (injury control). **(A–D)** Representative images for PEF-treated monolayers after 0–72 h. **(E–H)** Representative images for mechanically injured monolayers after 0–72 h. The initial scratch area was purposely made to be similar to that due to PEF. Scale bar: 2 mm. Cell monolayer boundaries of the injuries are outlined manually on the individual images.

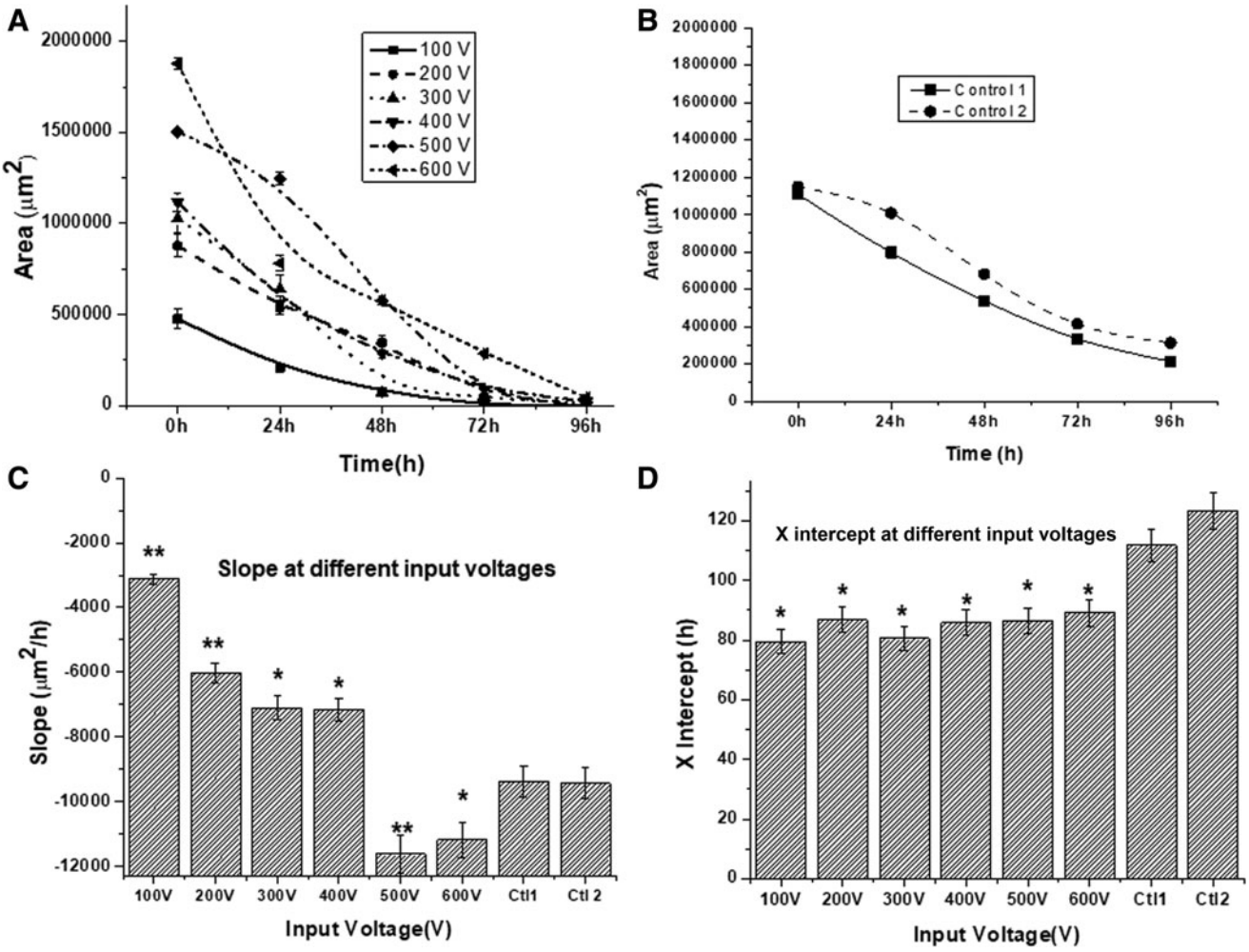

FIG. 3. Monolayer scratch injury area recovery as a function of time for fibroblasts (HFB). **(A)** Recovery plots after applying voltages ranging from 100 to 600 V, 2 mm apart. **(B)** Recovery plots for two scratch injuries in fibroblast monolayers compared with the initial injury area post-500–600 V PEF. **(C)** Comparison of slopes (representing average rate of healing) obtained from the recovery kinetics of fibroblasts shown in **(A, B)**. **(D)** Comparison of horizontal intercepts obtained from recovery kinetics of fibroblasts shown in **(A, B)**. Data are represented as mean ± standard deviation, $n = 3$. $^{*}p \leq 0.05$ and $^{**}p \leq 0.001$ with respect to control.

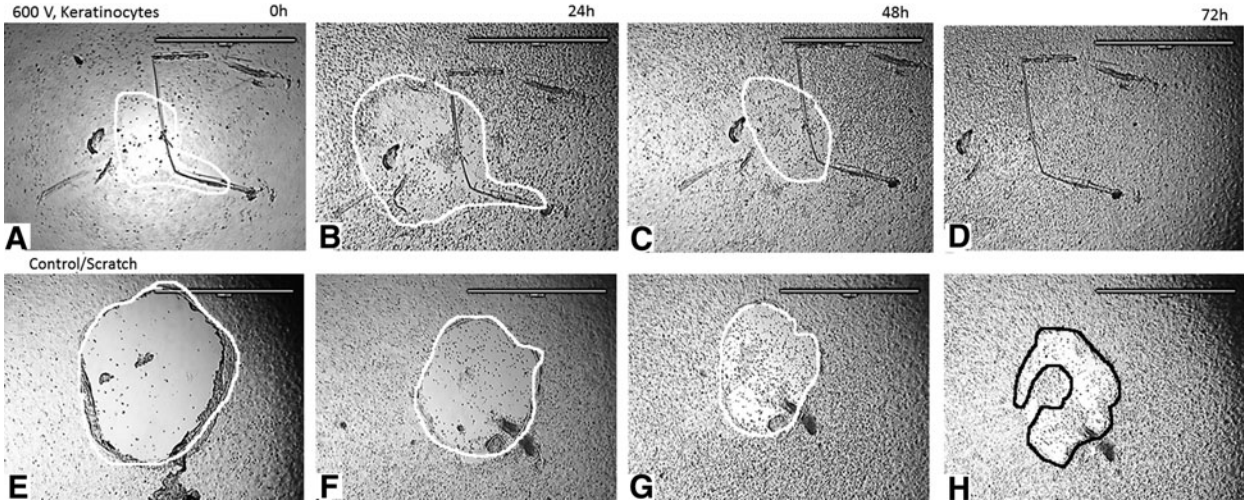

FIG. 4. Injury recovery of keratinocyte monolayers after treatment with 600 V PEF 2 mm apart, or after mechanical scratching (injury control). **(A–D)** Representative images for PEF-treated monolayers after 0–72 h. **(E–H)** Representative images for mechanically injured monolayers after 0–72 h. The initial scratch area was purposely made to be similar to the injury area post 24 h after application of PEF of 500–600 V voltage range. Scale bar: 2 mm. Cell monolayer boundaries of the injuries are outlined manually on the individual images.

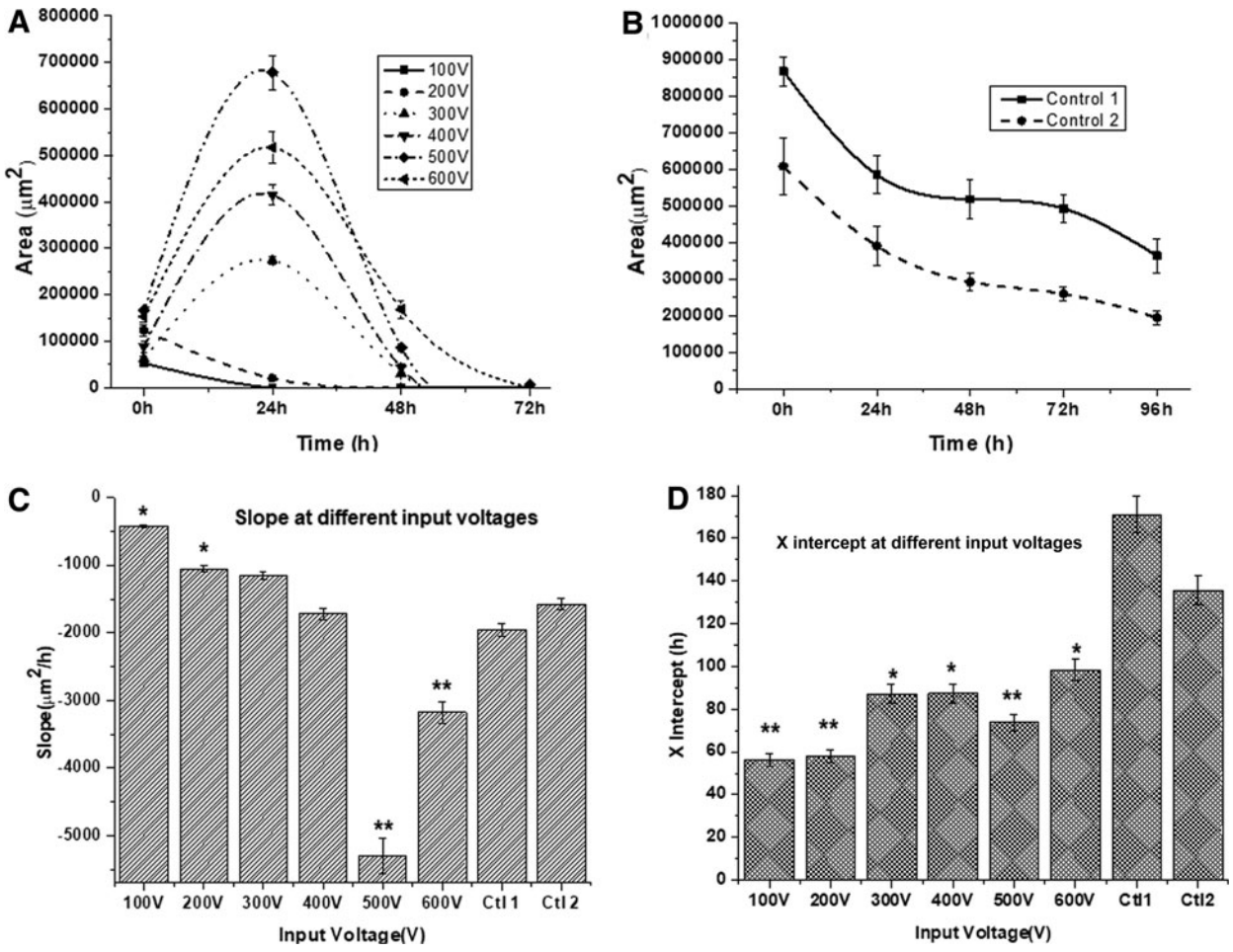

FIG. 5. Monolayer scratch area recovery as a function of time for keratinocytes. **(A)** Recovery plots after applying different voltages ranging from 100 to 600 V, 2 mm apart. **(B)** Recovery plots for two scratch injuries in keratinocyte monolayers having areas comparable to the injury area 24 h post-PEF (500–600 V). **(C)** Comparison of slopes (representing average rate of healing) obtained from the recovery kinetics of fibroblasts at different PEF intensities and two mechanical scratch controls shown in **(A, B). (D)** Comparison of horizontal intercepts obtained from recovery kinetics of fibroblasts at different PEF intensities and two mechanical scratch controls shown in **(A, B)**. Data are represented as mean ± standard deviation, $n = 3$. $^{*}p \leq 0.05$ and $^{**}p \leq 0.001$ with respect to the control.

horizontal (X axis) intercepts of the linear fitted plots of the area recovery curves, which represent the predicted time of closure of the injury.

Detection of ECM deposition post-PEF/mechanical injury

To determine whether PEF-mediated cell removal left some ECM behind, we electroporated (500 V between 2 mm) monolayers of both cell types, washed the monolayers thrice with PBS, and fixed them with 4% paraformaldehyde. Hematoxylin solution (Thermo Fisher) was added onto the sample for 5 min and washed with deionized water thrice. A negative control of mechanical scratch injury was also treated the same way. Color changes were visualized after exposing the samples to 1% acid alcohol for 30 s, followed by staining using Eosin solution (Thermo Fisher) for 2 min, and a three-time wash with deionized water. The samples were dehydrated using an ethanol gradient series. The control for this experiment consisted of cell monolayers killed by exposure to pure deionized water for 1 h and stained by the protocol mentioned above. All samples were imaged using an Olympus microscope with a color camera and images were further processed using ImageJ.

Effect of conditioned media on cells

To collect conditioned media, fibroblasts and keratinocyte monolayers were exposed to PEF as before using 500 V between 2 mm. After PEF and washing of PEF buffer with PBS three times, fresh and warm complete medium was added to the cultures. After 24 h, the conditioned media were collected and applied onto mechanically scratched monolayers of the same cell type. Control media samples from cells that were mechanically scratched over a similar area using a 200 μL micropipette tip (MS) were collected and applied. Additional controls consisted of spent media samples collected from untreated (UT) cell monolayers. Thus, the conditioned media study consisted of six different groups: PEF-fibroblasts to UT fibroblasts, MS-fibroblasts to UT fibroblasts, UT fibroblasts to UT fibroblasts, PEF-keratinocytes to UT keratinocytes, MS-keratinocytes to UT keratinocytes and UT keratinocytes to UT keratinocytes. The monolayer recovery was monitored at 24, 48, and 72 h.

Statistical analysis and curve fitting

All the results are reported as mean ± standard deviation with sample size $n = 3$, unless indicated otherwise. Student's t-test and analysis of variance were used to evaluate the significance of differences. At least $p \leq 0.05$ was considered statistically significant.

Results

Cell monolayer recovery after injury by PEF

The effect of simultaneous cellular ablation and stimulation by a nonuniform electric field was studied by applying voltages ranging from 100 to 600 V (between 2 mm) DC in electric pulses of 70 μs duration with a frequency of 1 Hz at a

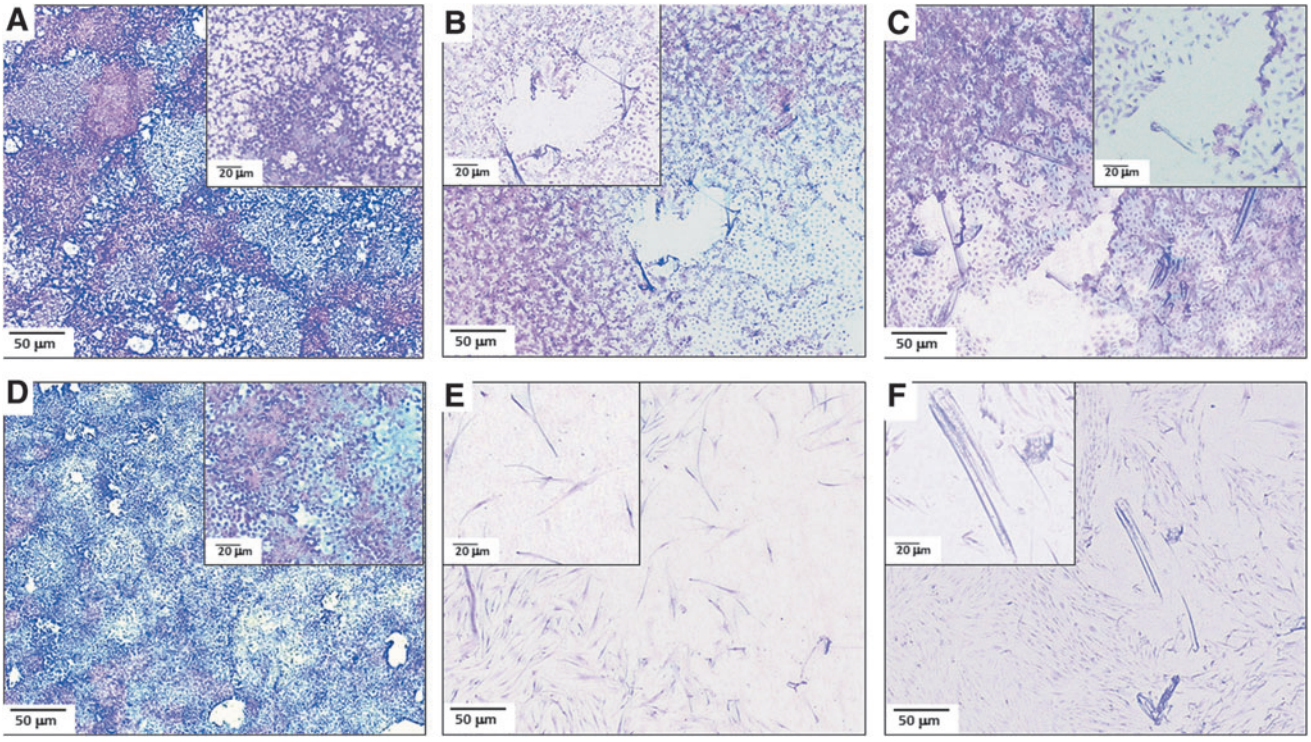

FIG. 6. Comparative morphology of cell monolayers after PEF-induced injury (500 V, 2 mm apart) or mechanical injury. Monolayers were fixed and stained with Hematoxylin and Eosin. **(A)** Keratinocyte control monolayer after exposure to deionized water to lyse cells while keeping ECM on the surface. **(B)** Keratinocyte monolayer after PEF. **(C)** Keratinocyte monolayer after mechanical injury. **(D)** Fibroblast control monolayer after exposure to deionized water. **(E)** Fibroblast monolayer after PEF. **(F)** Fibroblast monolayer after mechanical injury. Scale bar 50 μm. Inset higher magnification images provided: scale 20 μm. ECM, extracellular matrix.

very short distance above monolayers of fibroblasts or keratinocytes. The effect of PEF on the monolayer morphology was assessed over the course of 96 h.

To determine if this post-PEF behavior resulted from the application of a simulated mechanical wound to the monolayer, a scratch wound of approximately equal size was created. Recoveries of individual monolayers of fibroblasts and keratinocytes to both injury types were compared. In the case of fibroblasts (Fig. 2), the PEF treated cells (600 V applied 2 mm apart) appeared to repopulate the PEF-induced dead zone area (Fig. 2A–D) faster than the mechanically injured cellular monolayer (Fig. 2E–H).

Next, we carried out a voltage dose–response between 100 and 600 V (Fig. 3A). When using fibroblast monolayers, increasing voltage generally led to increased initial injury area, which then decreased in size as a function of time. The rate of decrease was fastest initially and then slowed down as the wound area approached zero at 72–96 h. Controls consisting of monolayers with initial mechanical scratch areas similar to that observed with 600 V PEF exhibited a constant rate of decrease until the wound was nearly closed at 96 h (Fig. 3B).

The slope analysis represents the rate of monolayer recovery at different PEF intensities compared with scratch injury controls. In the case of fibroblasts (Fig. 3C), for 500 and 600 V, where the initial injury area is comparable to the initial area of mechanical injury controls, the recovery rate was significantly higher than controls. However, at lower PEF intensities (100–400 V) the recovery rate was lower compared with mechanical injury. The horizontal intercept value provides an estimate of the time of wound closure (Fig. 3D). The wound closure time between different PEF voltages did not change significantly, but was much lower than mechanical injury controls (72–80 vs. >100 h).

Keratinocytes are another predominant skin cell type involved in wound healing. Therefore, we analyzed keratinocyte responses to PEF, where comparably sized injuries were created through PEF (600 V), which were also compared with mechanically scratched monolayers (Fig. 4). PEF-treated keratinocyte monolayers increased wound size between 0 and 24 h post-PEF, after which wound size decreased until disappearance. In contrast, mechanical scratch injuries monotonically decreased in size as a function of time. Thus, while PEF-treated keratinocyte monolayers underwent further wound opening in the first 24 h, subsequent recovery was more rapid than mechanically injured controls. When the PEF and mechanical injury wound area recovery was compared,

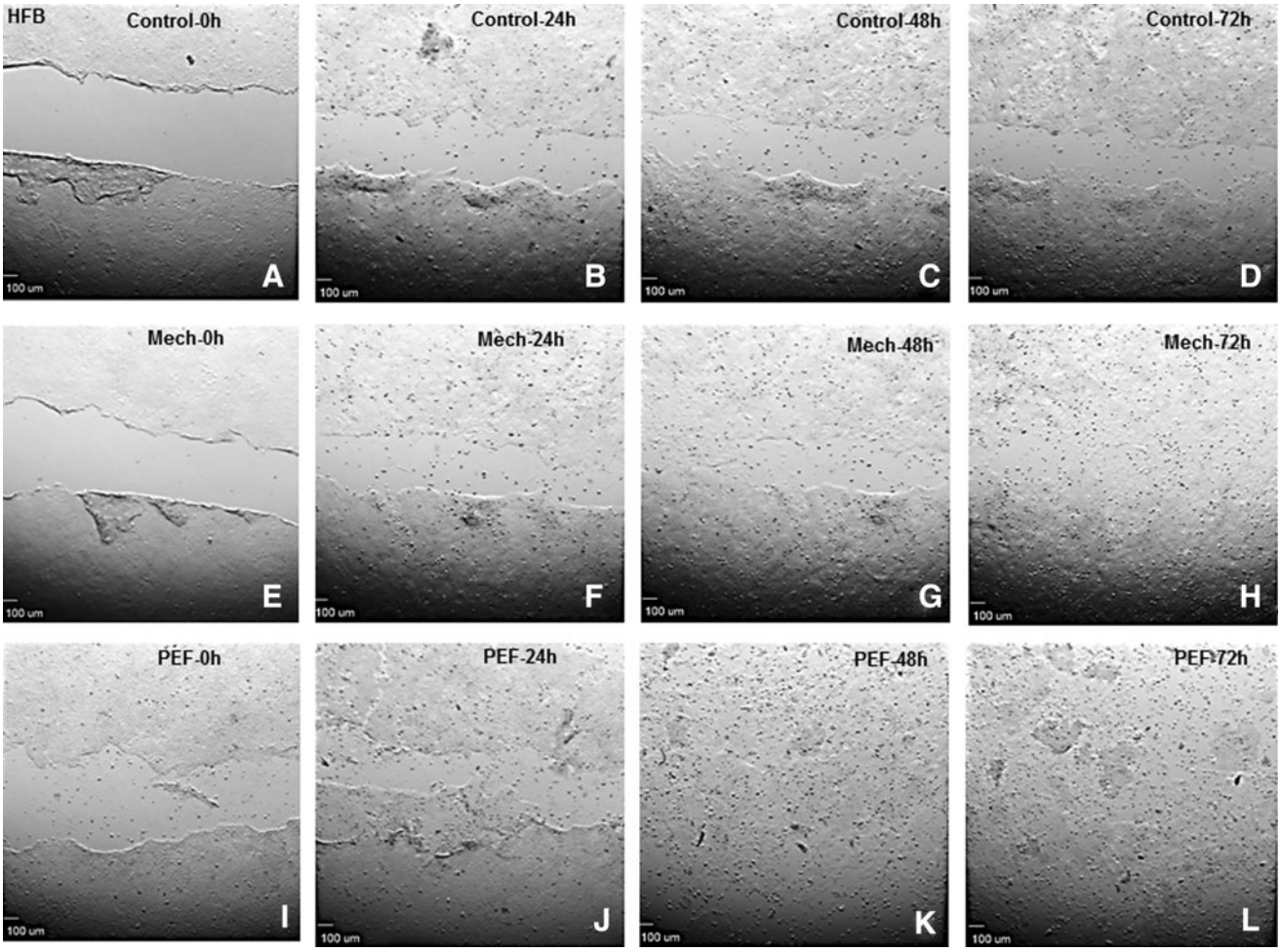

FIG. 7. Effect of conditioned media (collected 24 h post PEF application) on recovery of scratch wounds in fibroblast monolayers. **(A–D)** Samples exposed to conditioned media from untreated cells. **(E–H)** Samples exposed to conditioned media from mechanically scratched cells. **(I–L)** Samples exposed to conditioned media from containing PEF-treated cells.

the complete recovery time was observed to be within 72 h for PEF and >96 h for mechanical injury (Fig. 5A, B).

Next, we quantified the postinjury recovery for voltages ranging from 100 to 600 V. Except for the lowest intensities (100 and 200 V), a biphasic response was seen where wound area initially increased, followed by a decrease at 24 h post-PEF and beyond (Fig. 5A). The quickest injury recovery was observed when 500 V was applied (Fig. 5B).

To further compare and clarify the effect of PEF versus mechanical injury, both the slope and horizontal intercept for different PEF voltages and mechanical scratch injuries were calculated after fitting straight lines to the curves obtained above (Fig. 5C, D).

Similar trends for slope and intercept were also observed for keratinocytes. However, the rate of recovery around 500–600 V was much higher compared with the other PEF intensities and mechanical scratch controls (Fig. 5C). The estimated wound closure times among different PEF voltages did not vary significantly (Fig. 5D), but were collectively much lower than mechanical injury controls (70–90 vs. >140 h). Given these results, 500 V PEF applied 2 mm apart appears to be optimal for both cell types (recovery rate/slope = 11,200 μm^2/h in fibroblasts and 7000 μm^2/h in keratinocytes).

Mechanism analysis for enhanced cell growth after PEF

We hypothesized that enhanced cell growth post-PEF application may be attributed to either remaining ECM as guiding adherent cues or soluble molecular cues, which may signal neighboring cell infiltration.[27] Thus, PEF-treated monolayers were stained for ECM deposition, and the post-PEF-conditioned media were evaluated for its ability to promote cellular proliferation.

First, we assessed ECM deposition post-PEF or mechanical injury. For both keratinocytes and fibroblasts, no significant

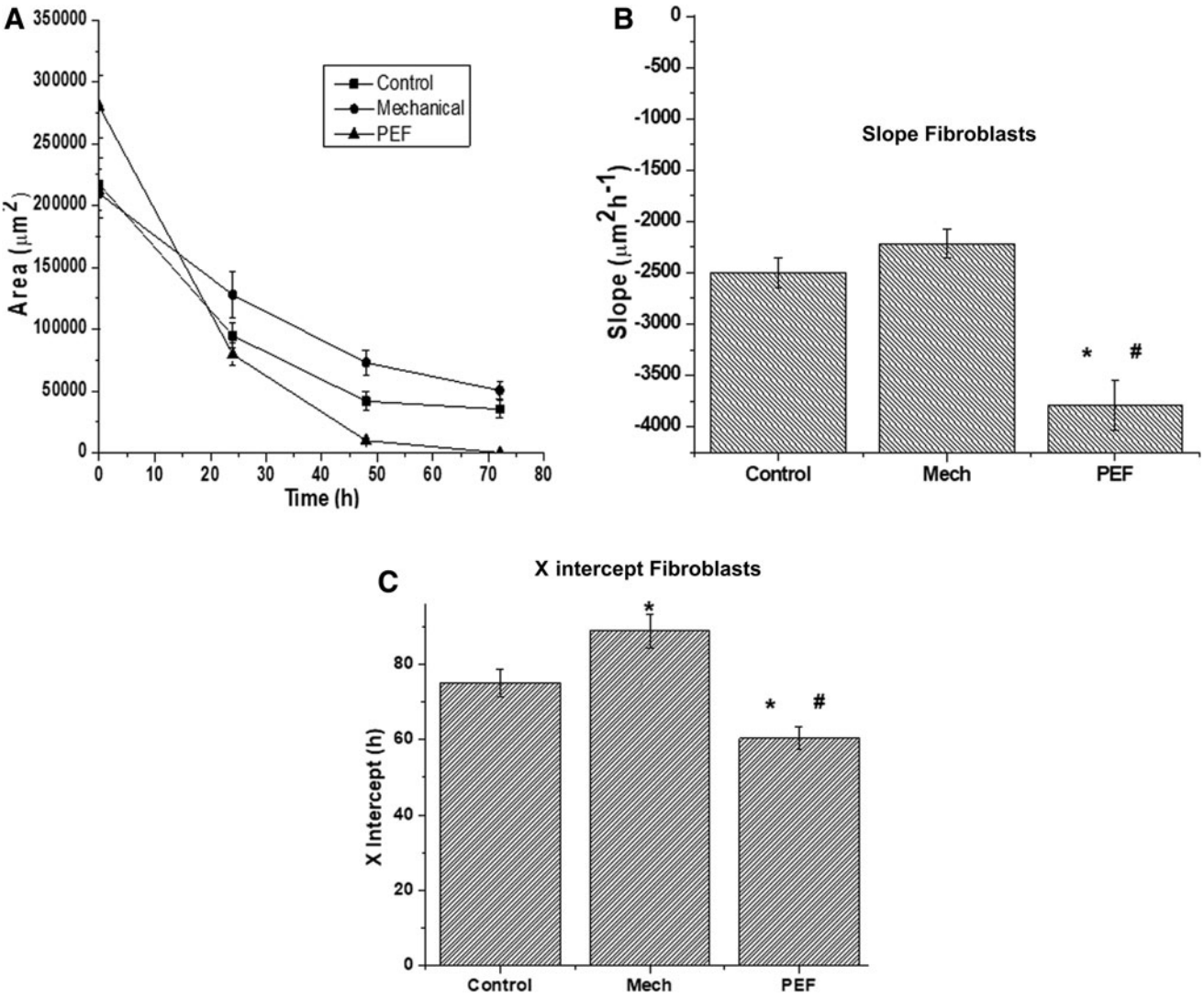

FIG. 8. Effect of conditioned media from PEF-treated or mechanically scratched cells on scratched responder monolayers. **(A)** Wound area recovery as a function of time in the presence of different conditioned media in fibroblasts. **(B)** Comparison of slopes (rate) of the recovery plot under influence of different conditioned media (fibroblasts). **(C)** Comparison of horizontal intercepts (probable complete recovery time) of the recovery plot under influence of different conditioned media (fibroblasts) ($^*p \leq 0.05$ with respect to control [untreated 24 h spent media] and $^{\#}p \leq 0.05$ with respect to mechanical injury).

remaining protein was observed (Fig. 6B, E), which was also the case with mechanical injury (Fig. 6C, F). These results suggest that nominal to negligible ECM remains post-PEF indicating that deposited ECM is not likely a major factor in the recovery of monolayers after PEF treatment. In contrast, protein deposits were clearly visible after hypotonic lysis (Fig. 6A, D).

Next, we tested the potential of soluble factors secreted in conditioned media obtained from cellular monolayers post-PEF treatment to promote the healing of standard mechanically scratched responder cells (both fibroblasts and keratinocytes). Three different groups were used to generate conditioned media: (1) intact UT monolayers, (2) mechanically injured monolayers (injury control), and (3) 500 V PEF injured monolayers. Conditioned media were collected after 24 h incubation and applied onto responded cells of the same type. In the case of fibroblasts (Fig. 7), it was evident that recovery of the scratch injury was fastest in PEF-conditioned media (within 48 h) followed by mechanical injury-conditioned and UT monolayer-conditioned media.

We quantifed this response by comparing the area of recovery versus time for fibroblasts (Fig. 8A), and confirmed that PEF-conditioned media caused the responder cells to heal much faster (90% closure within the first 48 h). Furthermore, the slope (Fig. 8B), which reflects the rate of recovery, was significantly steeper ($\sim 3900\ \mu m^2/h$) compared to that for mechanical injury ($\sim 2000\ \mu m^2/h$) and UT monolayers ($\sim 2600\ \mu m^2/h$). The horizontal intercept (Fig. 8C), used to estimate the wound closure time, was also the lowest for the PEF-conditioned media group.

When a similar experiment was conducted with keratinocytes (Fig. 9), PEF-conditioned media were also found to promote the fastest wound healing response in the responder cells (Fig. 10B) (PEF: $6000\ \mu m^2/h$, mechanical injury: $2900\ \mu m^2/h$ and UT monolayer $3500\ \mu m^2/h$). The estimated wound closure time was also the shortest with PEF-conditioned media (Fig. 10C).

Discussion

Our objective was to combine the lethal and stimulatory effects of PEF upon two major skin cells, dermal fibroblasts, and keratinocytes. We observed that both fibroblasts and keratinocytes are affected by strong nonuniform PEF. High-intensity PEF killed almost all of the cells at the center of the electrodes leaving an open injury. While rapid cell death was

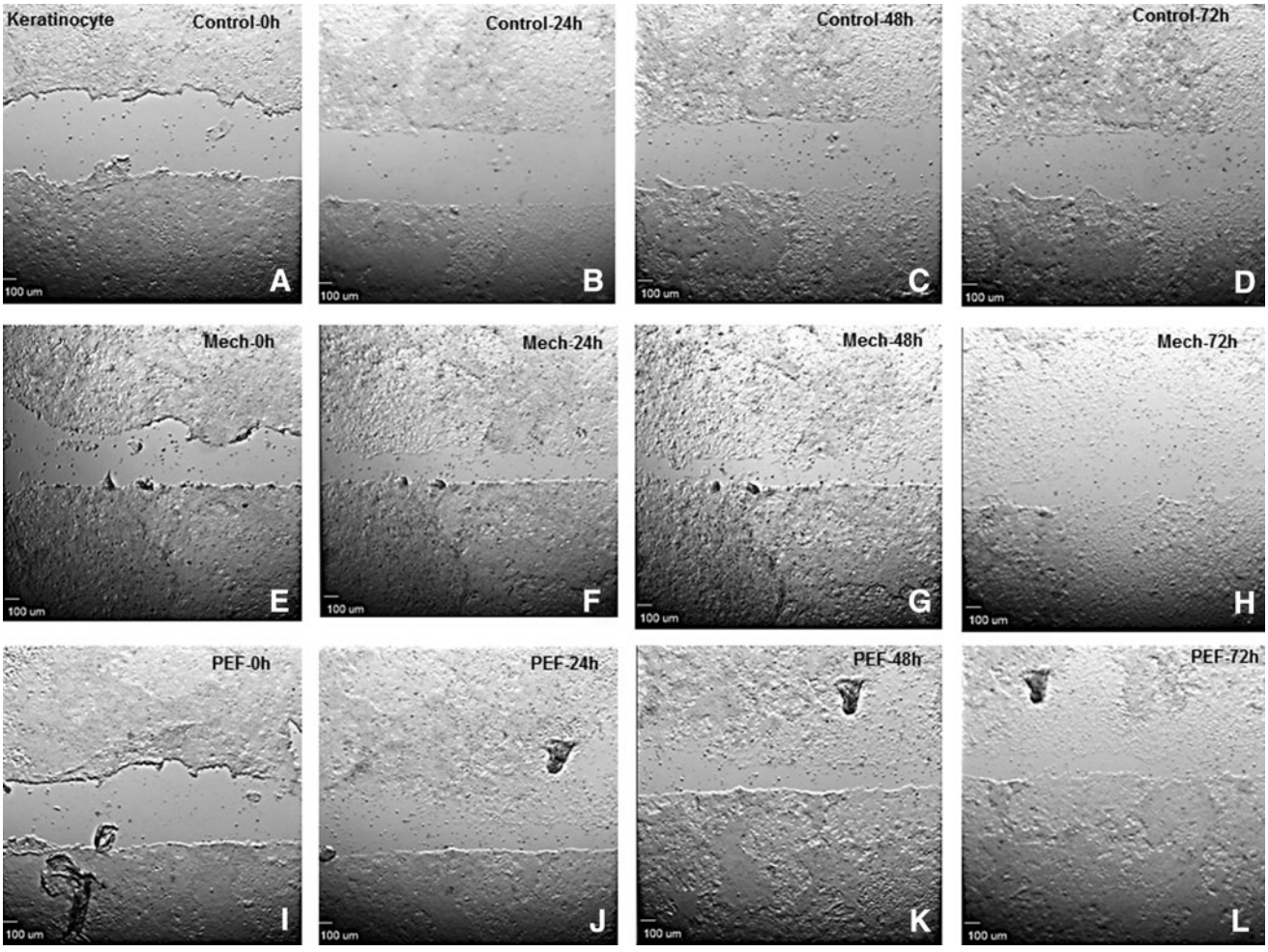

FIG. 9. Effect of conditioned media (collected 24 h post PEF application) on recovery of scratch wounds in keratinocyte monolayers. **(A–D)** Samples exposed to conditioned media from untreated cells. **(E–H)** Samples exposed to conditioned media from mechanically scratched cells. **(I–L)** Samples exposed to conditioned media from containing PEF-treated cells.

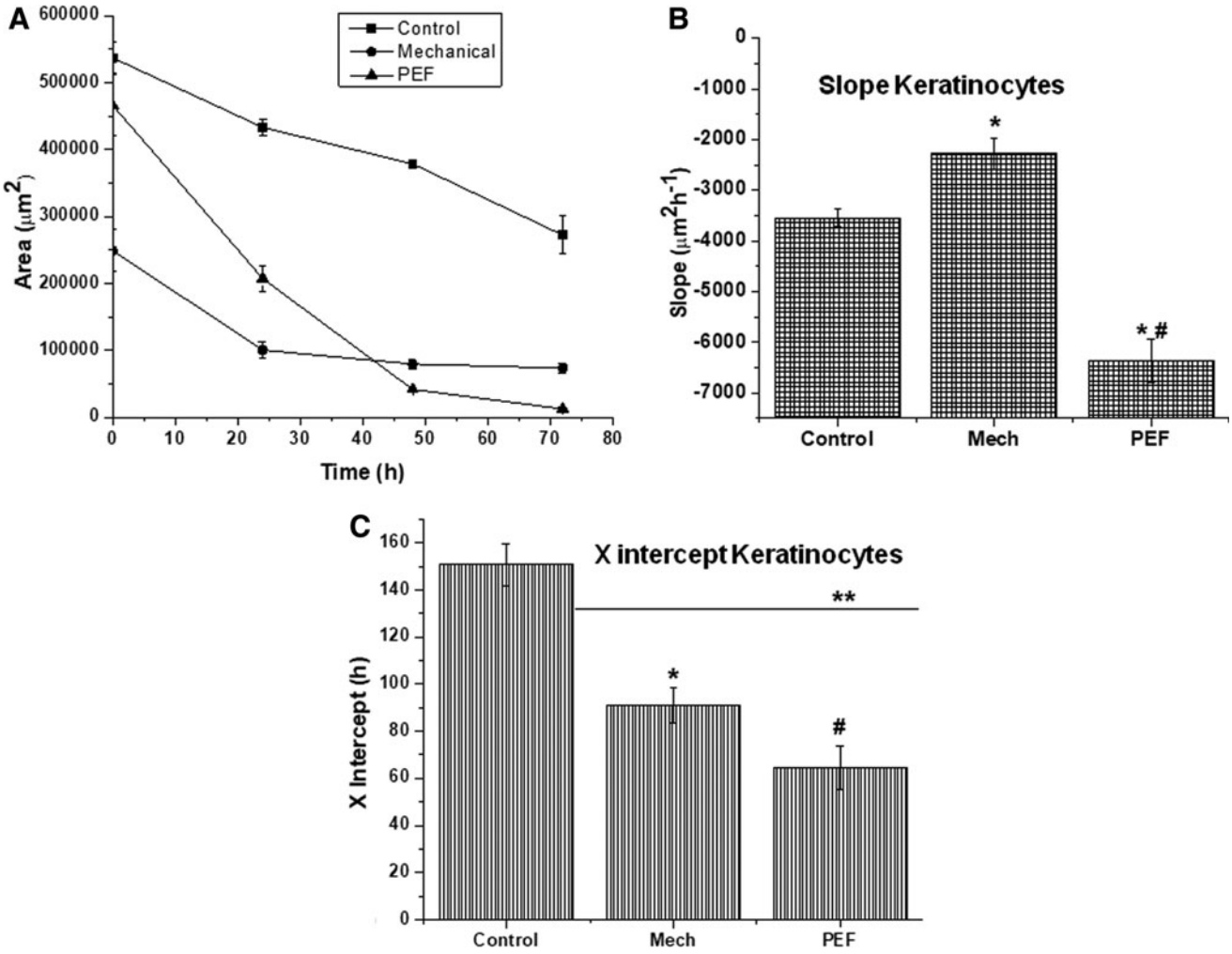

FIG. 10. Quantification of the effect of conditioned media (24 h post PEF application) on recovery of scratch wounds in keratinocyte monolayers. **(A)** Wound area decreases as a function of time in the presence of different conditioned media. **(B)** Comparison of slopes (rate of wound closure) for the different conditioned media. **(C)** Comparison of *X* intercepts (estimated wound closure time) for the different conditioned media. $^{*}p \leq 0.05$ and $^{**}p \leq 0.001$ with respect to conditioned media from untreated monolayers, and $^{\#}p \leq 0.05$ with respect to conditioned media from mechanical injury.

expected to take place in the center, in the area where the PEF intensity was below the lethal dose, the cells were observed to infiltrate into the open area more rapidly compared with a mechanical scratch injury of similar size (Figs. 2 and 4).[28] This demonstrates that nonuniform PEF can create a dual effect of cell death and cell stimulation.[26]

PEF induces nanopores by altering the cell membrane potential, which can activate multiple biological pathways.[29] PEF is also known to generate reactive oxygen species, which also work as secondary messengers and can contribute to a delayed cell death mechanism.[30,31] Our current study indicates that there is delayed cell death in keratinocyte monolayers, which is followed by rapid recovery post PEF application. This phenomenon was completely absent in mechanical injuries. Therefore, application of PEF can affect both death and growth patterns of fibroblasts and keratinocytes, which is critical for wound healing.

Prior studies used high-intensity short-duration PEF as a means to ablate or kill cells or tissues,[18,32,33] or low-intensity long-duration PEF for tissue stimulation to heal injuries.[34,35] Herein, we bridge the gap between these two phenomena. Thus, nonuniform PEF can potentially be used for injured tissue removal (PEF-mediated debridement) as well as to signal nearby healthy cells to infiltrate. We determined an optimal applied voltage (500 V applied 2 mm apart), which increased the wound closure rate for both cell types we characterized (fibroblasts and keratinocytes) compared with mechanical scratch injuries (Fig. 5). However, we observed very different cell death and regrowth responses between the two cell types. After PEF, fibroblasts followed a monotonous pattern of healing with generally linear kinetics of wound closure. The major impact on fibroblasts of PEF compared with scratch injury was the shorter healing time (Fig. 3). In contrast, immediately after PEF administration to keratinocytes, an injury area developed, which increased in size over the first 24 h, in a form of delayed cell death (Figs. 4 and 5). After this phase, the growth rate of keratinocytes was enhanced drastically. Cell growth eventually slowed when approaching wound closure.

PEF induces nanopores by altering the cell membrane potential, which can activate multiple biological pathways.[29]

PEF is also known to generate reactive oxygen species, which also work as secondary messengers and can contribute to a delayed cell death mechanism.[30,31] These pathways may explain the differences between PEF and mechanical injuries in keratinocytes.[36] It is, however, unclear why fibroblasts did not exhibit delayed injury after PEF, an observation which may warrant further study.

Recently, it has been observed that PEF treatment could help skin and liver regeneration with little scar tissue formation.[15,16,37] Application of PEF (500 V/mm) and higher number of pulses (1000 pulses) have also been observed to promote scarless healing and preserve secondary organs of skin like hair follicles in rodent models.[17] While it has been postulated that PEF kills only cells keeping the tissue ECM architecture intact leading to less scar formation, the exact mechanism that controls these processes is not yet well understood. This *in vitro* study suggests that leftover ECM is not the major driving force for rapid recovery post PEF. We observed little to no sparing of the ECM on the surface after PEF, as well as mechanical scratch injury (Fig. 6). However, we observed that soluble factors released into the media may be more important contributors to the unusual stimulatory effect of PEF on woud healing *in vitro*. Furthermore, if we compare the slopes (rate) for PEF-treated fibroblasts and keratinocytes, we observed a faster recovery rate in keratinocytes (fibroblasts: 3900 μm^2/h and keratinocytes 6000 μm^2/h). Thus, soluble factors present in conditioned media due to PEF treatment might have a bigger impact on keratinocytes than fibroblasts. This may explain the faster recovery of PEF-treated keratinocytes compared with fibroblasts in our studies.

Conclusion

In summary, we observed that nonuniform electric fields can be useful for cell destruction and cell growth simultaneously. Interestingly, the application of PEF may favor keratinocytes over fibroblasts. Fibroblasts were more prone to PEF-induced cell death relative to keratinocytes. The recovery rates of PEF-induced keratinocytes were also observed to be faster with respect to fibroblasts both in direct PEF application as well as secondarily, through application of conditioned media. Further exploration of the application of PEF to different *in vitro* models would enable us to better understand the underlying mechanisms of previously reported improved *in vivo* wound healing after PEF in skin and other tissues.[16,38]

Author Contributions

F.B.: experimental planning, experimental design, article writing and editing. B.D.: study planning, experimental design, experimental execution, data analysis, article writing and editing. A.G.: experimental planning and article editing. R.S.: experimental planning, experimental design, article writing and editing. A.S.: experimental design, article editing. M.L.Y.: experimental design, article editing. All coauthors have reviewed and approved this article before submission. This article has been submitted solely to this journal and is not published, in press, or submitted elsewhere.

Author Disclosure Statement

No competing financial interests exist.

Funding Information

This work was partially supported by the New Jersey Commission for Spinal Cord Research (grants No. CSCR17ERG006 and CSCR20FEL013), and the US–Israel Binational Science Foundation (grant No. 2017129).

References

1. Saulis G. Electroporation of cell membranes: The fundamental effects of pulsed electric fields in food processing. Food Eng Rev 2010;2:52–73.
2. Buckow R, Ng S, Toepfl S. Pulsed electric field processing of orange juice: A review on microbial, enzymatic, nutritional, and sensory quality and stability. Compr Rev Food Sci Food Saf 2013;12:455–467.
3. Madison AC, Royal MW, Vigneault F, et al. Scalable Device for Automated Microbial Electroporation in a Digital Microfluidic Platform. ACS Synth Biol 2017;6:1701–1709.
4. Golzio M, Teissie J, Rols MP. Cell synchronization effect on mammalian cell permeabilization and gene delivery by electric field. Biochim Biophys Acta 2002;1563:23–28.
5. Narayanan G. Irreversible electroporation. Semin Intervent Radiol 2015;32:349–355.
6. Ivey JW, Wasson EM, Alinezhadbalalami N et al. Characterization of ablation thresholds for 3D-cultured patient-derived glioma stem cells in response to high-frequency irreversible electroporation. Research 2019;2019:8081315.
7. Mi Y, Li P, Liu Q, et al. Multi-parametric study of the viability of in vitro skin cancer cells exposed to nanosecond pulsed electric fields combined with multi-walled carbon nanotubes. Technol Cancer Res Treat 2019;18: 1533033819876918.
8. Novickij V, Cesna R, Perminaite E, et al. Antitumor response and immunomodulatory effects of sub-microsecond irreversible electroporation and its combination with calcium electroporation. Cancers 2019;11:1763.
9. Gibot L, Golberg A. Electroporation in scars/wound healing and skin response. In: Miklavcic D, ed. Handbook of Electroporation. Cham: Springer International Publishing, 2016: 1–18.
10. Aaron RK, Ciombor DM. Therapeutic effects of electromagnetic fields in the stimulation of connective tissue repair. J Cell Biochem 1993;52:42–46.
11. Golberg A, Broelsch GF, Vecchio D, et al. Eradication of multidrug-resistant A. baumannii in burn wounds by antiseptic pulsed electric field. Technology 2014;2:153–160.
12. Golberg A, Broelsch GF, Vecchio D, et al. Pulsed electric fields for burn wound disinfection in a murine model. J Burn Care Res 2015;36:7–13.
13. Barki KG, Das A, Dixith S, et al. Electric field based dressing disrupts mixed-species bacterial biofilm infection and restores functional wound healing. Ann Surg 2019;269: 756–766.
14. Maor E, Ivorra A, Leor J, et al. The effect of irreversible electroporation on blood vessels. Technol Cancer Res Treat 2007;6:307–312.
15. Golberg A, Khan S, Belov V, et al. Skin rejuvenation with non-invasive pulsed electric fields. Sci Rep 2015;5:10187.
16. Golberg A, Broelsch GF, Bohr S, et al. Non-thermal, pulsed electric field cell ablation: A novel tool for regenerative medicine and scarless skin regeneration. Technology 2013; 1:1–7.
17. Golberg A, Villiger M, Felix Broelsch G, et al. Skin regeneration with all accessory organs following ablation

with irreversible electroporation. J Tissue Eng Regen Med 2018;12:98–113.
18. Golberg A, Yarmush ML. Nonthermal irreversible electroporation: Fundamentals, applications, and challenges. IEEE Transact Biomed Eng 2013;60:707–714.
19. Tai G, Tai M, Zhao M. Electrically stimulated cell migration and its contribution to wound healing. Burns Trauma 2018;6:20.
20. Tyler SEB. Nature's electric potential: A systematic review of the role of bioelectricity in wound healing and regenerative processes in animals, humans, and plants. Front Physiol 2017;8:627.
21. Ross CL. The use of electric, magnetic, and electromagnetic field for directed cell migration and adhesion in regenerative medicine. Biotechnol Prog 2017;33:5–16.
22. Zimolag E, Borowczyk-Michalowska J, Kedracka-Krok S, et al. Electric field as a potential directional cue in homing of bone marrow-derived mesenchymal stem cells to cutaneous wounds. Biochim Biophys Acta Mol Cell Res 2017; 1864:267–279.
23. Aoki M, Matsumoto NM, Okubo Y, et al. Cytochrome P450 genes play central roles in transcriptional response by keratinocytes to a high-voltage alternating current electric field. Bioelectrochemistry 2019;126:163–171.
24. Cho Y, Son M, Jeong H, et al. Electric field-induced migration and intercellular stress alignment in a collective epithelial monolayer. Mol Biol Cell 2018;29:2292–2302.
25. Castle J, Garner AL, Smith RD, et al. Hematopoietic stem cell and fibroblast proliferation following platelet electrostimulation. IEEE Access 2018;6:56395–56401.
26. Vadlamani RA, Nie Y, Detwiler DA, et al. Nanosecond pulsed electric field induced proliferation and differentiation of osteoblasts and myoblasts. J R Soc Interface 2019; 16:20190079.
27. Chang TT, Zhou VX, Rubinsky B. Using non-thermal irreversible electroporation to create an in vivo niche for exogenous cell engraftment. Biotechniques 2017;62:229–231.
28. Robinson VS, Garner AL, Loveless AM, et al. Calculated plasma membrane voltage induced by applying electric pulses using capacitive coupling. Biomed Phys Eng Express 2017;3:025016.
29. Cao Y, Ma E, Cestellos-Blanco S, et al. Nontoxic nanopore electroporation for effective intracellular delivery of biological macromolecules. Proc Natl Acad Sci U S A 2019; 116:7899.
30. Minamitani Y, Kobayashi Y, Kageyama R. Investigation of difference of origin of ROS generated in a cell by frequency components of pulsed electric field. In: 2015 IEEE Pulsed Power Conference (PPC), Austin, TX, 2015:1–4.
31. Pakhomova ON, Khorokhorina VA, Bowman AM, et al. Oxidative effects of nanosecond pulsed electric field exposure in cells and cell-free media. Arch Biochem Biophys 2012;527:55–64.
32. Chen R. Nanosecond pulsed electric field (nsPEF) Ablation as an alternative or adjunct to surgery for treatment of cancer. Surg Curr Res 2013;S12:005.
33. Nuccitelli R. Practical applications of bioelectric stimulation. Bioelectricity 2019;1:203.
34. Thakral G, LaFontaine J, Najafi B, et al. Electrical stimulation to accelerate wound healing. Diabet Foot Ankle 2013;4:22081.
35. Nuccitelli R. Nano-pulse stimulation therapy for the treatment of skin lesions. Bioelectricity 2019;1:235–239.
36. Beebe SJ. Cell responses without receptors and ligands, using nanosecond pulsed electric fields (nsPEFs). Int J Nanomedicine 2013;8:3401–3404.
37. Golberg A, Bruinsma BG, Jaramillo M, et al. Rat liver regeneration following ablation with irreversible electroporation. PeerJ 2016;4:e1571.
38. Li X, Saeidi N, Villiger M, et al. Rejuvenation of aged rat skin with pulsed electric fields. J Tissue Eng Regen Med 2018;12:2309–2318.

Address correspondence to:
Martin L. Yarmush, MD, PhD
Department of Biomedical Engineering
Rutgers University
599 Taylor Road
Piscataway, NJ 08854
USA

Email: yarmush@soe.rutgers.edu